DOI: https://doi.org/10.54338/27382656-2022.2-005

Lan Hoang That Ton
HCMC University of Architecture, HCMC, Vietnam

THREE KINDS OF POROSITY ON FUNCTIONALLY GRADED POROUS BEAMS

In this paper, the effects of three types of porosity on bending behavior of functionally graded porous (FGP) beams are studied. The procedure of finite element method (FEM) is established and based on the simple Timoshenko beam theory. The results achieved in this paper are presented and compared with other results in the references to verify the feasibility of implementing the formula and writing the Matlab code. On the other hand, this paper can help researchers to have an overview of the bending behavior of the FGP beams.

***Keywords**: bending behavior, functionally graded porous (FGP) beam, transverse displacement, rotation, simple Timoshenko beam.*

Introduction

Nowadays, functionally graded (FG) material has become one of the smart materials and it is used in many countries. From a mixture of ceramic and metal, it provided a continuous variation of material properties from the top surface to the bottom surface of a structure. For example, some structures like nuclear tanks, spacecraft, etc. are produced based on the above material [1-3]. Due to the high applicability of FG material, many studies related to various theories have been given to comment the mechanical behavior of FG structures as [4-9]. However, porosity of the material can occur during the manufacturing process [10-12]. So, for a good knowledge of porosity effect on bending behavior of FG structures, a study related to this issue must be considered as soon as possible. There are three types of structure, like beam, plate and shell, but researchers are usually interested in beam structures because of its wide applications. Furthermore, many different beam theories were used to analyze beam structures, like simple beam theory [13], classical beam theory [14, 15], first-order shear deformation theory [16-20] or higher-order shear deformation theory [21, 22]. However, using a simple Timoshenko beam model helps us to reduce the computational cost with the resulting error within the allowable range. On the other hand, beams made of FGP materials should be investigated as much as possible to help the designer have the right knowledge about the mechanical properties. The few published papers on static bending behavior of FG beams can be listed here. Author Chen and co-workers presented the Ritz method to obtain the transverse bending deflections and critical buckling loads, where the trial functions take the form of simple algebraic polynomials [23]. A novel model was introduced for bending of FGP cantilever beams by [24] related to shape memory alloy/poroelastic composite material. In this article, the authors verified the accuracy of the bending model by a three-dimensional (3D) finite element method (FEM). Another paper based on trigonometric shear deformation theory was used to analyze the bending, vibration and buckling characteristics of FGP graphene-reinforced nanocomposite curved beams from [25], and so on. From above reasons, this paper is given to investigate the bending behavior of FGP beams.

This paper has four parts. Part 1 gives the introduction as above. Part 2 presents the formulations as well as Part 3 shows some essential results. Finally, a few comments are also given in Part 4, respectively.

Formulations

A FGP beam with length L, width b and thickness h is considered. Three forms of porosity distributions are studied and shown in Figures 1 and 2, in which (*1*) is uniform porous distribution and (*2*) and (*3*) are non-uniform porous distributions respectively. The normalized Young's modulus $E(z)/E_1$ is depicted in Fig. 2 (a) - (c) to clarify the influences of these three forms of porosity with the value of Young's modulus at top surface, E_1.

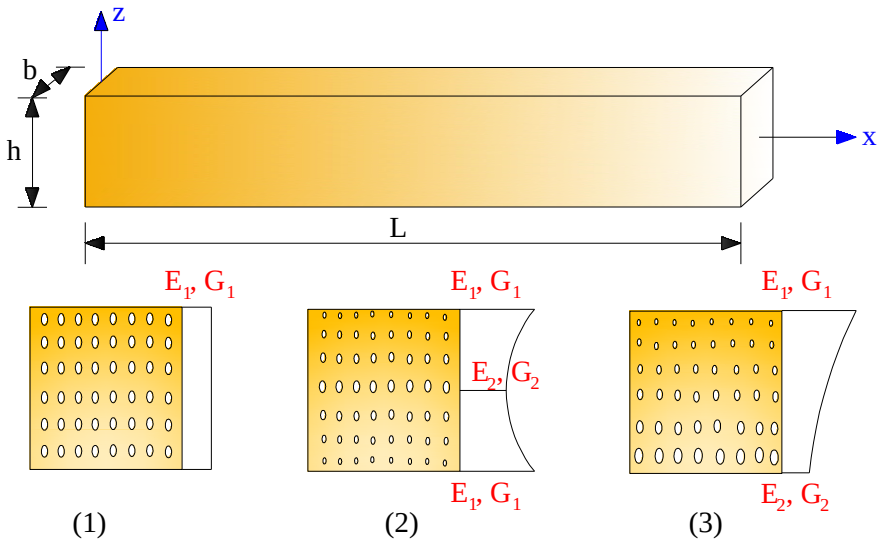

Fig. 1. *FGP beam with three types of porosity 1, 2 and 3*

The material properties such as Young's modulus, $E(z)$, and shear modulus, $G(z)$, can be described as below:

$$\begin{cases} E(z) = E_1(1 - e_0\chi) \\ G(z) = G_1(1 - e_0\chi) \end{cases} \quad \text{with} \quad \chi = \frac{1}{e_0} - \frac{1}{e_0}\left(\frac{2}{\pi}\sqrt{1-e_0} - \frac{2}{\pi} + 1\right)^2 \quad \text{for type (1)} \tag{1}$$

$$\begin{cases} E(z) = E_1\left(1 - e_0 \cos\left(\frac{\pi z}{h}\right)\right) \\ G(z) = G_1\left(1 - e_0 \cos\left(\frac{\pi z}{h}\right)\right) \end{cases} \quad \text{for type (2)} \tag{2}$$

$$\begin{cases} E(z) = E_1\left(1 - e_0 \cos\left(\frac{\pi z}{2h} + \frac{\pi}{4}\right)\right) \\ G(z) = G_1\left(1 - e_0 \cos\left(\frac{\pi z}{2h} + \frac{\pi}{4}\right)\right) \end{cases} \quad \text{for type (3)} \tag{3}$$

The porosity coefficient e_0 must satisfy $0 < e_0 < 1$ and

$$e_0 = 1 - \frac{E_2}{E_1} = 1 - \frac{G_2}{G_1}. \tag{4}$$

Based on FEM, the degrees of freedom associated with a node of a simple Timoshenko beam element are a transverse displacement and a rotation as depicted in Fig. 3. Using the principles of simple beam theory, the beam element stiffness matrix $\mathbf{K}_{el}$ will be derived

$$\mathbf{K}_{el} = \frac{E_{el} I_{el}}{L_{el}^3} \begin{bmatrix} 12/(1+\Xi) & 6L_{el}/(1+\Xi) & -12/(1+\Xi) & 6L_{el}/(1+\Xi) \\ 6L_{el}/(1+\Xi) & (4+\Xi)L_{el}^2/(1+\Xi) & -6L_{el}/(1+\Xi) & (2-\Xi)L_{el}^2/(1+\Xi) \\ -12/(1+\Xi) & -6L_{el}/(1+\Xi) & 12/(1+\Xi) & -6L_{el}/(1+\Xi) \\ 6L_{el}/(1+\Xi) & (2-\Xi)L_{el}^2/(1+\Xi) & -6L_{el}/(1+\Xi) & (4+\Xi)L_{el}^2/(1+\Xi) \end{bmatrix} \tag{5}$$

with

$$\Xi = (12E_{el}I_{el})/(G_{el}sA_{el}L_{el}^2), \tag{6}$$

s =5/6 is called the shear correct factor; E_{el}, G_{el} and I_{el} are Young's modulus, shear modulus and second moment of area of element based on $E(z)$, $G(z)$, b and h; L_{el} is length of element and A_{el} is called the area of cross section.

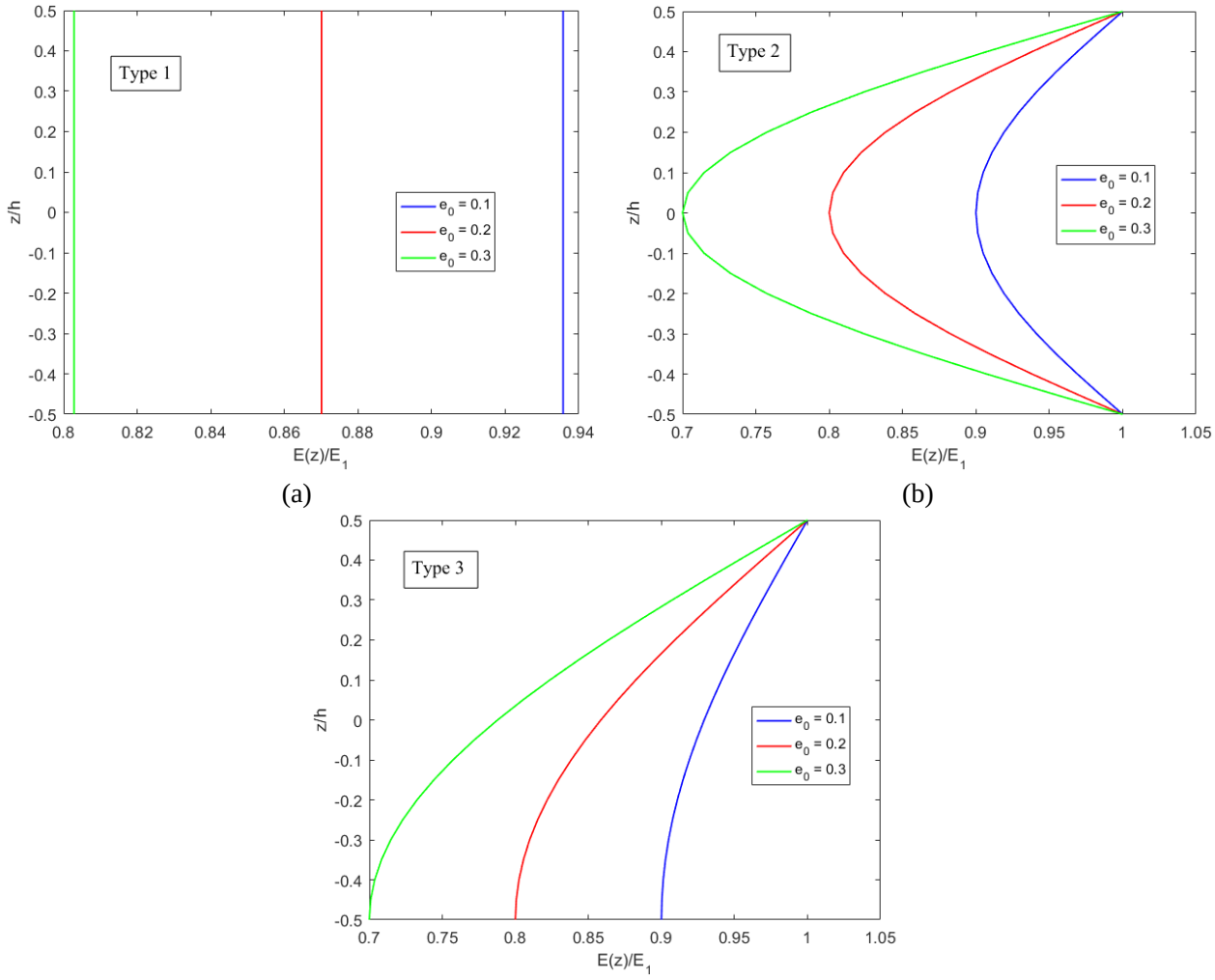

Fig. 2. *Normalized material property E(z)/E₁ with (a) type 1, (b) type 2 and (c) type 3 of porosity*

According to the principle of minimum total potential energy, the element equation can be described as

$$\frac{E_{el}I_{el}}{L_{el}^3}\begin{bmatrix} 12/(1+\Xi) & 6L_{el}/(1+\Xi) & -12/(1+\Xi) & 6L_{el}/(1+\Xi) \\ 6L_{el}/(1+\Xi) & (4+\Xi)L_{el}^2/(1+\Xi) & -6L_{el}/(1+\Xi) & (2-\Xi)L_{el}^2/(1+\Xi) \\ -12/(1+\Xi) & -6L_{el}/(1+\Xi) & 12/(1+\Xi) & -6L_{el}/(1+\Xi) \\ 6L_{el}/(1+\Xi) & (2-\Xi)L_{el}^2/(1+\Xi) & -6L_{el}/(1+\Xi) & (4+\Xi)L_{el}^2/(1+\Xi) \end{bmatrix}\begin{Bmatrix} w_i \\ \varphi_i \\ w_j \\ \varphi_j \end{Bmatrix} = \begin{Bmatrix} f_i \\ m_i \\ f_j \\ m_j \end{Bmatrix} \quad (7)$$

After assembly, the bending variables can be obtained by solving the following equation:

$$\mathbf{K}_{total}\,\mathbf{d}_{total} = \mathbf{F}_{total} \quad (8)$$

Fig. 3. *Two nodes* ***i*** *and* ***j*** *of a beam element*

By using three letters **C**, **S** and **F** refer to the clamped, simply supported and free condition, all boundary conditions can be revealed as below (Fig.4).

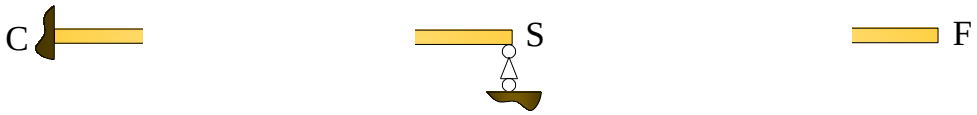

Fig. 4. *Three types of boundary condition*

From Fig. 4, the boundary conditions of system can be presented:

$$w(0)=\varphi(0)=0\ ,\ w(L)=0 \qquad \text{for CS} \tag{9}$$

$$w(0)=\varphi(0)=0\ ,\ w(L)=\varphi(L)=0 \qquad \text{for CC} \tag{10}$$

$$w(0)=\varphi(0)=0 \qquad \text{for CF} \tag{11}$$

More clearly, the finite element system of equations can be reached as below

Input data: material and geometrical properties,

Calculating constitutive matrix,

Loop over elements: calculating element stiffness matrix $\mathbf{K}_{el}$ and element force vector $\mathbf{F}_{el}$,

Assembling all parts in the global coordinate system to have $\mathbf{K}_{total}$ and $\mathbf{F}_{total}$,

Applying boundary conditions CS, CC or CF,

Solving equation to achieve $\mathbf{d}_{total}$,

Display transverse displacements w and rotations φ at nodes of system.

Numerical Examples

Firstly, the validity of the proposed model is checked for (CC) and (CS) isotropic beams under a uniform load $q = 10^6$ N/m^2. The material and geometric properties are $E = 1$ GPa, $v = 1/3$, $b = 0.1$ m, $h = 0.1$ m and $L = 10h$. The maximum transverse displacement and rotation as in the Table below are calculated and compared with analytical solutions [26] as follows:

(CC)

$$w=\frac{1}{EI}\left[\frac{1}{24}qL^2x^2-\frac{1}{12}qLx^3+\frac{1}{24}qx^4\right] \tag{12}$$

$$\varphi=\frac{1}{EI}\left[\frac{1}{12}qL^2x-\frac{1}{4}qLx^2+\frac{1}{6}qx^3\right] \tag{13}$$

(CS)

$$w=\frac{1}{48EI}\left[-3qL^2x^2+5qLx^3-2qx^4\right] \tag{14}$$

$$\varphi=\frac{1}{48EI}\left[-6qL^2x+15qLx^2-8qx^3\right] \tag{15}$$

It can be seen that the results obtained from the paper are completely approximate with other results. The relative error among above results can be explained by using different approaches.

Table. The comparison of the maximum transverse displacements at position $x = L/2$ of (SS) isotropic beams with $L/h = 5$

	$w_{\max}$		$\varphi_{\max}$	
CC	Analytical	Paper	Analytical	Paper
	0.3125	0.3126	0.9375	0.9383
	$w_{\max}$		$\varphi_{\max}$	
CS	Analytical	Paper	Analytical	Paper
	0.6480	0.6466	1.7187	1.7002

Secondly, the material of the porous beam is assumed to be steel foam with E_1 = 200 GPa, ν = 1/3. The cross section of beam is h = 0.1 m, b = 0.1 m . The normalized maximum deflections $\bar{w} = w_{\max} / h$ based on this study for two boundary conditions (CC) and (CS) are compared with other results of [23] as in Fig. 5. Again, their convergence proves the reliability of the proposed method in bending analysis of FGP beams.

Thirdly, by changing the boundary condition from (CC) to (CS) and (CF), the bending behaviors of FGP beams can be seen in Fig. 6 (a) - (c) for three types 1, 2 and 3. Once again, the effects of porosity on the bending behavior of this structure are clearly presented in these Figures. Furthermore, Fig. 7 depicts the influence of porosity on the deflections of (CF) porous beams for type 1, type 2 and type 3 respectively.

Finally, by varying the porosity coefficient e_0, the length to thickness ratio L/h and three types 1, 2 and 3, the results of the normalized transverse displacement $\bar{w} = w(L/2)/h$ at position $L/2$ of FGP beams with (CC) boundary condition are plotted in Fig. 8 (a) - (c). As the porosity value increases, the deflection of FGP beam also increases and this statement holds for all cases.

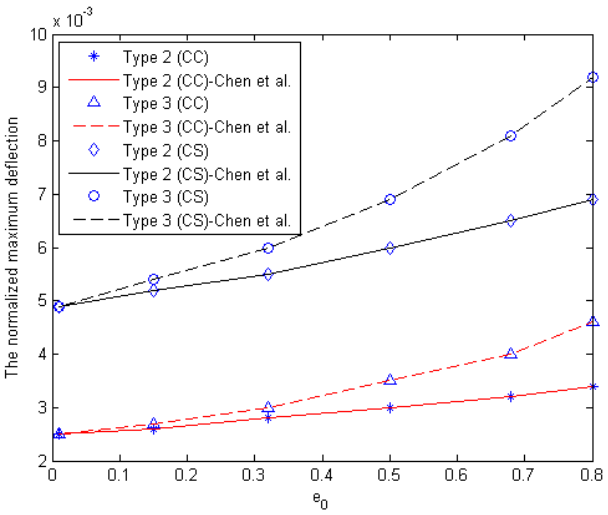

Fig. 5. *Convergence of the deflection*

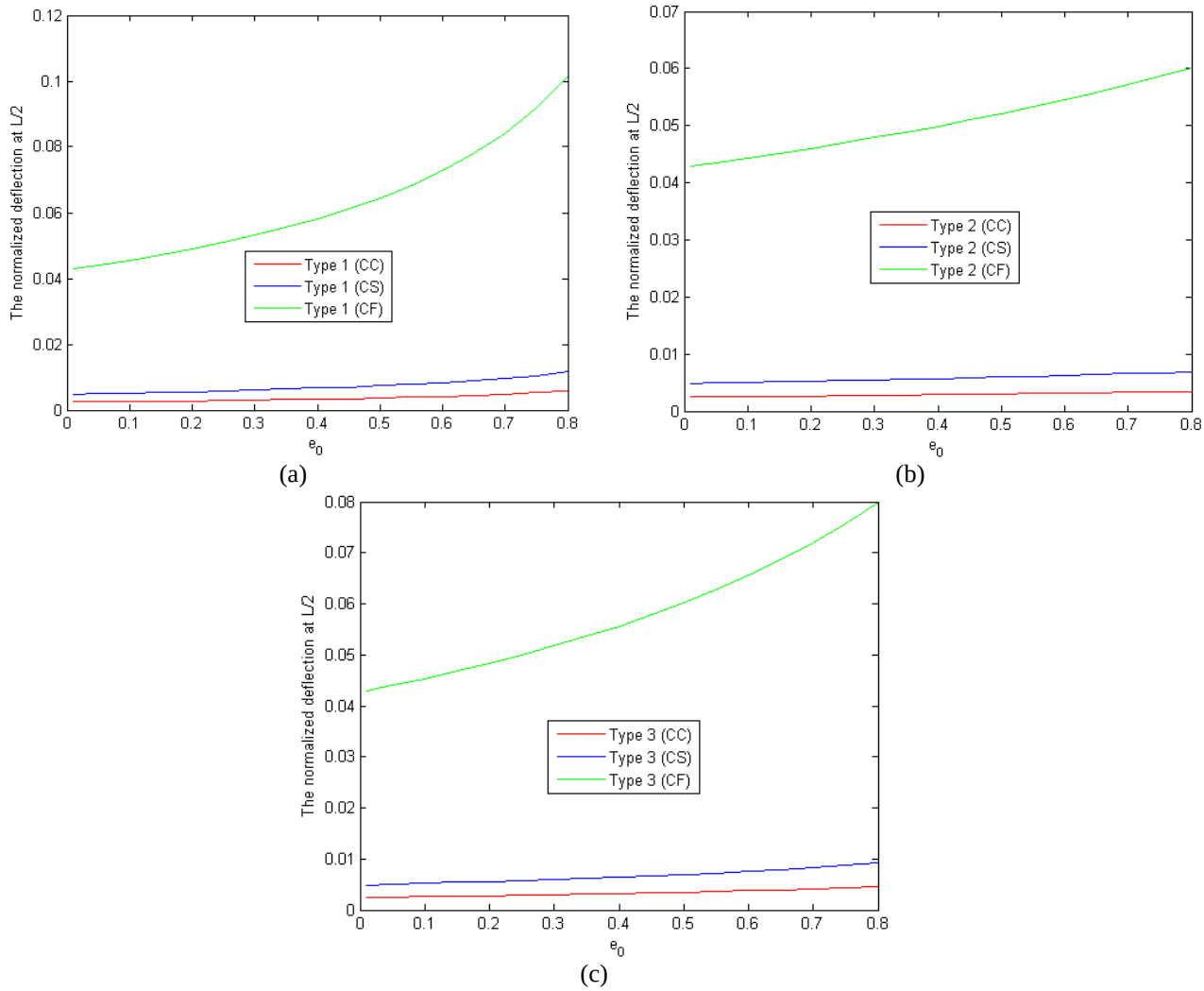

Fig. 6. *The influence of e_0 on the deflections of porous beams with (a) type 1 / (b) type 2 / (c) type 3 for three boundary conditions*

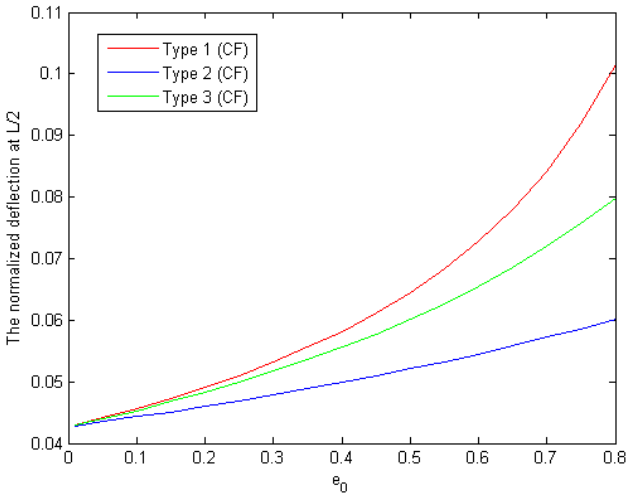

Fig. 7. *The influence of e_0 on the deflection of (CF) porous beam with three types 1, 2 and 3*

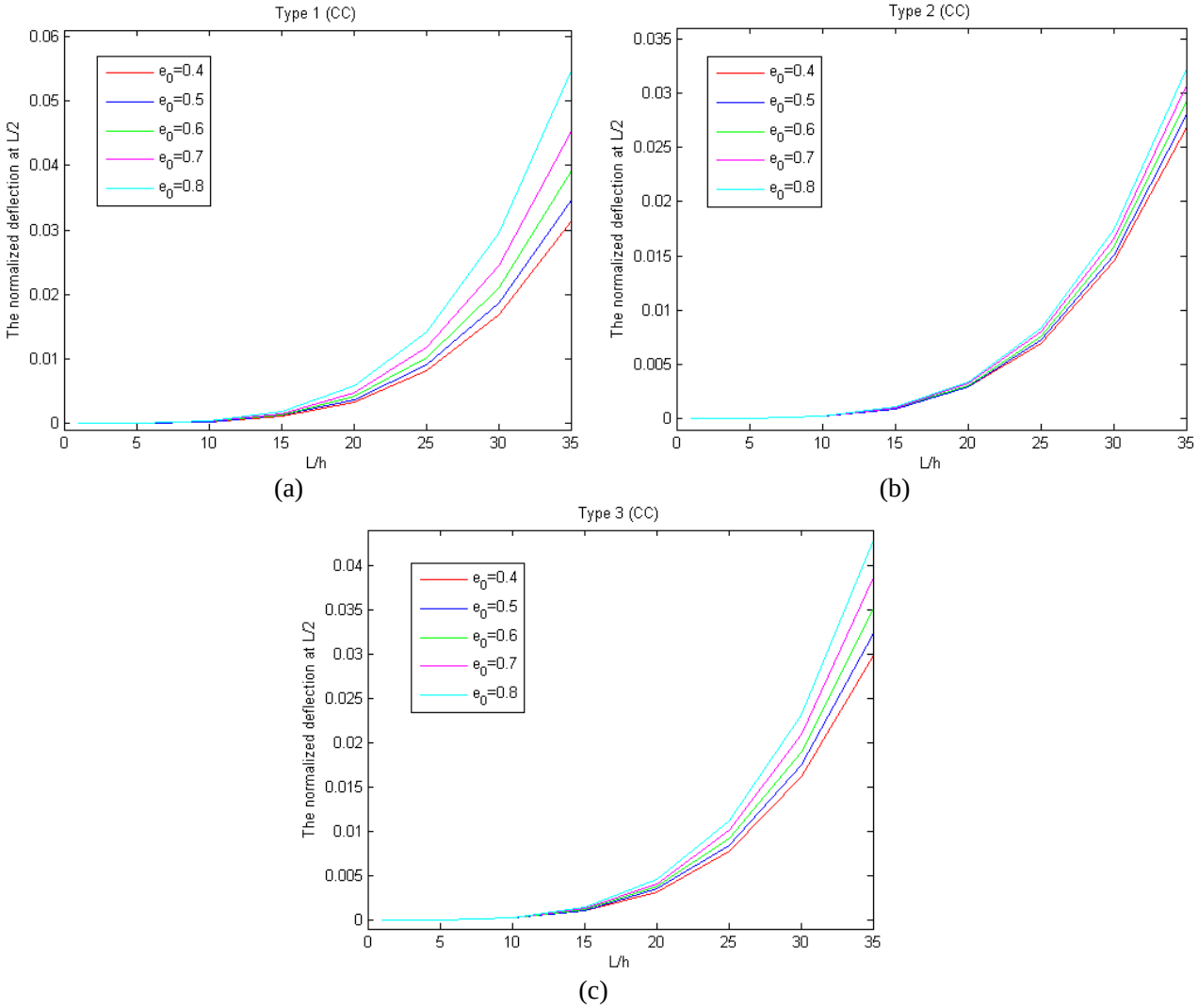

Fig. 8. *The deflections of (a) type 1 / (b) type 2 / (c) type 3 (CC) porous beams by changing ratio L/h and porosity factor e_0*

Conclusion

The bending behaviors of FGP beams under three different types of boundary condition and three kinds of porosity are presented in this study. The verification results based on this Matlab code are in good agreement

with other results in reference and the main goal of the author is to demonstrate the applicability of simple theory to analyzing the FGP beams with acceptable results.

Conflicts of Interest

No conflict of interest was declared by the author.

References

[1]. O. Carvalho, M. Buciumeanu, G. Miranda, S. Madeira, F.S. Silva, Development of a Method to Produce Fgms by Controlling the Reinforcement Distribution. Materials & Design, 92, 2016, 233-239.
[2]. R.K. Singh, V. Rastogi, A Review on Solid State Fabrication Methods and Property Characterization of Functionally Graded Materials. Materials Today: Proceedings, 2021.
[3]. V. Boggarapu, R. Gujjala, S. Ojha, S. Acharya, P. Venkateswara babu, S. Chowdary et al., State of the Art in Functionally Graded Materials. Composite Structures, 262, 2021, 113596.
[4]. M. Gautam, M. Chaturvedi, Optimization of Functionally Graded Material under Thermal Stresses. Materials Today: Proceedings, 44, 2021, 1520-1523.
[5]. M. Sam, R. Jojith, N. Radhika, Progression in Manufacturing of Functionally Graded Materials and Impact of Thermal Treatment - A Critical Review. Journal of Manufacturing Processes, 68, 2021, 1339-1377.
[6]. Y. Mognhod Bezzie, D. Engida Woldemichael, E. Tefera Chekol, S. Alemneh Admass, S.K. Selvaraj, V. Paramasivam, Effect of Volumetric Fraction Index on Temperature Distribution in Thick-Walled Functionally Graded Material Made Cylinder. Materials Today: Proceedings, 46, 2021, 7442-7447.
[7]. H. Liu, S. Ding, B.F. Ng, Impact Response and Energy Absorption of Functionally Graded Foam Under Temperature Gradient Environment. Composites Part B: Engineering, 172, 2019, 516-532.
[8]. V.N. Burlayenko, H. Altenbach, T. Sadowski, S.D. Dimitrova, A. Bhaskar, Modelling Functionally Graded Materials in Heat Transfer and Thermal Stress Analysis by Means of Graded Finite Elements. Applied Mathematical Modelling, 45, 2017, 422-438.
[9]. Z. Zheng, Y.Yi, X. Bai, A. Nakayama, Functionally Graded Structures for Heat Transfer Enhancement. International Journal of Heat and Mass Transfer, 173, 2021, 121254.
[10]. Y. Xiong, Z. Han, J. Qin, L. Dong, H. Zhang, Y. Wang et al., Effects of Porosity Gradient Pattern on Mechanical Performance of Additive Manufactured Ti-6Al-4V Functionally Graded Porous Structure. Materials & Design, 208, 2021, 109911.
[11]. M. Iasiello, N. Bianco, W.K.S. Chiu, V. Naso, The Effects of Variable Porosity and Cell Size on the Thermal Performance of Functionally-Graded Foams. International Journal of Thermal Sciences, 160, 2021, 106696.
[12]. G.H. Loh, E. Pei, D. Harrison, M.D. Monzón, An Overview of Functionally Graded Additive Manufacturing. Additive Manufacturing, 23, 2018, 34-44.
[13]. S.R. Singiresu, The Finite Element Method in Engineering. Elsevier, 2018.
[14]. X.F. Li, A Unified Approach for Analyzing Static and Dynamic Behaviors of Functionally Graded Timoshenko and Euler–Bernoulli Beams. Journal of Sound and Vibration, 318, 2008, 1210-1229.
[15]. D. Wu, W. Gao, D. Hui, K. Gao, K. Li, Stochastic Static Analysis of Euler-Bernoulli Type Functionally Graded Structures. Composites Part B: Engineering, 134, 2018, 69-80.
[16]. I. Katili, T. Syahril, A.M. Katili, Static and Free Vibration Analysis of FGM Beam Based on Unified and İntegrated of Timoshenko's Theory. Composite Structures, 242, 2020, 112130.
[17]. S.-R. Li, D.-F. Cao, Z.-Q. Wan, Bending Solutions of FGM Timoshenko Beams from Those of the Homogenous Euler–Bernoulli Beams. Applied Mathematical Modelling, 37, 2013, 7077-7085.
[18]. H.L. Ton-That, H. Nguyen-Van, T. Chau-Dinh, A Novel Quadrilateral Element for Analysis of Functionally Graded Porous Plates/Shells Reinforced by Graphene Platelets. Archive of Applied Mechanics, 91, 2021, 2435-2466.
[19]. H.L. Ton-That, The Linear and Nonlinear Bending Analyses of Functionally Graded Carbon Nanotube-Reinforced Composite Plates Based on the Novel Four-Node Quadrilateral Element. European Journal of Computational Mechanics, 29 (1), 2020, 139-172.
[20]. M. Şimşek, T. Kocatürk, Ş.D. Akbaş, Static Bending of a Functionally Graded Microscale Timoshenko Beam Based on the Modified Couple Stress Theory. Composite Structures, 95, 2013, 740-747.
[21]. H.L. Ton-That, A Combined Strain Element to Functionally Graded Structures in Thermal Environment. Acta Polytechnica, 60 (6), 2020, 528-539.

[22]. P.V. Avhad, A.S. Sayyad, Static Analysis of Functionally Graded Composite Beams Curved in Elevation Using Higher Order Shear and Normal Deformation Theory. Materials Today: Proceedings, 21, 2020, 1195-1199.
[23]. D. Chen, J. Yang, S. Kitipornchai, Elastic Buckling and Static Bending of Shear Deformable Functionally Graded Porous Beam. Composite Structures, 133, 2015, 54-61.
[24]. N.V. Viet, W. Zaki, Bending Model for Functionally Graded Porous Shape Memory Alloy/ Poroelastic Composite Cantilever Beams. Applied Mathematical Modelling, 97, 2021, 398-417.
[25]. B. Anirudh, M. Ganapathi, C. Anant, O. Polit, A Comprehensive Analysis of Porous Graphene-Reinforced Curved Beams by Finite Element Approach Using Higher-Order Structural Theory: Bending, Vibration and Buckling. Composite Structures, 222, 2019, 110899.
[26]. G. Marcial, Mechanics of Materials. ed. Purdue University, 2021.

Lan Hoang That Ton *(Vietnam, HCMC) - HCMC University of Architecture, Faculty of Civil Engineering, Assistant Professor, tltechonlinesom@gmail.com*

Received: 13.06.2022
Revised: 20.06.2022
Accepted: 21.06.2022